Marine Chemistry 148 (2013) 44–51

Contents lists available at SciVerse ScienceDirect

Marine Chemistry

journal homepage: www.elsevier.com/locate/marchem

Combined effect of light exposure and microbial activity on distinct dissolved organic matter pools. A seasonal field study in an oligotrophic coastal system (Blanes Bay, NW Mediterranean)

Cristina Romera-Castillo [a,*], Xosé Antón Álvarez-Salgado [b], Martí Galí [a], Josep M. Gasol [a], Célia Marrasé [a]

[a] ICM-CSIC, Institut de Ciències del Mar, Passeig Maritim de la Barceloneta 37-49, 08003 Barcelona, Spain
[b] IIM-CSIC, Instituto de Investigacións Mariñas, Eduardo Cabello 6, 36208 Vigo, Spain

ARTICLE INFO

Article history:
Received 1 February 2012
Received in revised form 29 October 2012
Accepted 31 October 2012
Available online 10 December 2012

Keywords:
CDOM
FDOM
Microbiology
Photochemistry
Mediterranean Sea
Blanes Bay

ABSTRACT

A harmonic analysis of three years of data collected with fortnight to monthly frequency in the oligotrophic Bay of Blanes (NW Mediterranean) revealed that the water column mixing-stratification cycle dictated the seasonal build-up of the bulk and different coloured fractions of dissolved organic matter (DOM). Dissolved organic carbon (DOC) accumulated at late summer, reaching the annual maximum by early September, half a month later than water temperature. The seasonal cycle of the protein-like fluorescence ($F(280/350)$) was in phase with DOC, suggesting that reduced heterotrophic activity, due to severe P limitation, is likely the reason behind the late summer accumulation of these materials. The absorption due to conjugated carbon double bonds of DOM ($a_{CDOM}(254)$) reached the annual maximum by early August, concomitant to the seasonal maximum of microbial activity, suggesting that biological production prevailed over photo-degradation of these compounds. On the contrary, the fluorescence of humic-like substances absorbing in the UV-A region ($F(340/440)$) presented the annual maximum in early February, coinciding with the seasonal maximum of autotrophic biomass, and the minimum in early August, because of the prevalence of photo-degradation over microbial production. The optical properties of DOM allowed distinguishing between three DOC pools of contrasting origin, photo- and bio-reactivity, in the oligotrophic NW Mediterranean Sea.

1. Introduction

Coloured dissolved organic matter (CDOM) includes all dissolved organic compounds that absorb ultraviolet and visible radiation. It is the major factor controlling the attenuation of UV radiation in the ocean (Kirk, 1994), which affects both primary and bacterial production (Herndl et al., 1993; Smith and Cullen, 1995). The absorption properties of CDOM are due to the presence of conjugated carbon double bonds. When they form aromatic rings, part of the absorbed light may be emitted as fluorescence (Stedmon and Álvarez-Salgado, 2011). CDOM absorption coefficients and spectral slopes have been used as tracers of the chemical structure and origin of DOM in aquatic environments (Dahlén et al., 1996; Nelson et al., 2004; Helms et al., 2008). The C-specific decadic absorption coefficient at 254 nm, $SUVA_{254}$, has been found to be a good tracer for the aromaticity of aquatic humic substances (Weishaar et al., 2003) and the ratio of absorption coefficients at 254 and 365 nm, $a_{CDOM}(254/365)$, and absorption spectral slopes, have been used as indices of the average molecular weight of DOM (Dahlén et al., 1996; Engelhaupt et al., 2003; Helms et al., 2008). The fraction of CDOM that emits absorbed UV radiation as fluorescence is called fluorescent dissolved organic matter (FDOM). The concatenation of emission fluorescence spectra collected at different excitation wavelengths results in excitation emission matrices where different peaks, characteristics of humic- and protein-like compounds, can be distinguished (Coble, 1996). The peaks named as C, M and A are due to humic-like fluorophores, while peaks T and B are due to protein-like fluorophores. Fluorescence intensity measurements at these peaks can be used to follow the dynamics of different DOM pools. The fluorescence to absorption coefficient ratio at 340 nm, a proxy of the fluorescence quantum yield, has also been used as an aromaticity index (Birks, 1970; Turro, 1991).

The main biogeochemical processes affecting the optical properties of DOM are: photodegradation, which provokes a loss of absorption and fluorescence of humic-like materials (e.g., Del Castillo et al., 1999; Moran et al., 2000; Nieto-Cid et al., 2006); and biodegradation, which produces an increase of the absorption and fluorescence of humic-like compounds and a decrease of the fluorescence of protein-like compounds (e.g. Kramer and Herndl, 2004; Lønborg et al., 2010; Romera-Castillo et al., 2011a). In some cases, natural UV light can produce an increase of the fluorescence and absorption of both humic-like (Kieber et al., 1997) and protein-like compounds (Romera-Castillo et al., in prep). The study of absorption and fluorescence, as well as the indices obtained from them, allows to identify

* Corresponding author. Tel.: +34 93 230 9500; fax: +34 93 230 95 55.
E-mail address: crisrc@icm.csic.es (C. Romera-Castillo).

0304-4203/$ – see front matter © 2012 Published by Elsevier B.V.
http://dx.doi.org/10.1016/j.marchem.2012.10.004

and somewhat quantify, the main processes affecting DOM in aquatic systems. Despite the fact that fluorescence and absorption of DOM are two parameters that can easily be measured, information about the temporal variability of the CDOM and/or FDOM pools in time-series stations is still scarce (but see Nelson et al., 1998; Para et al., 2010).

The Blanes Bay Microbial Observatory (http://www.icm.csic.es/bio/projects/icmicrobis/bbmo/) is a reference station in the NW Mediterranean Sea placed 1 km offshore of the town of Blanes. These waters are oligotrophic and phosphorous limited for most of the year (Lucea et al., 2005). Rain and mixing episodes, frequent in autumn and early winter, are followed by a prolonged period of high atmospheric pressure. The associated well irradiated and calm waters in late winter act as the main seasonal trigger in the NW Mediterranean Sea, setting the development of phytoplankton blooms (Duarte et al., 1999; Guadayol et al., 2009). This station has been studied for a long period (e.g., Margalef, 1945; Gasol et al., 1995; Duarte et al., 1999) with special emphasis on microbial plankton ecology (e.g. Alonso-Sáez et al., 2008; Galand et al., 2010). The monthly sampling on this site since 1992 has resulted in an invaluable database to examine and test environmental issues. In this study, we took advantage of this data collection to investigate the seasonal cycles of different sub-fractions of the DOM pool through their optical properties and the physical and biogeochemical processes, photochemistry and microbial activity, conditioning their variability.

2. Materials and methods

2.1. Survey area and sampling strategy

The Blanes Bay Microbial Observatory (NW Mediterranean Sea, 41° 40′N, 2° 48′E), is located in the continental side of the shelf/slope front, between the submarine Blanes Canyon, placed in the north, and the mouth of the La Tordera River in the south. The bottom depth at the sampling station is 22 m.

Seawater samples for this project were taken with fortnightly to monthly frequency from March 2008 to March 2011. They were collected from the surface layer (0.5 m depth), pre-filtered through a 200 μm nylon mesh to remove larger mesozooplankton and transported to the base laboratory (Barcelona) in acid-washed 25 L polycarbonate carboys within 2 h. In situ water salinity and temperature were measured with a CTD model SAIV A/S SD204. Total irradiance was recorded hourly by a pyranometer in the nearby meteorological station of Malgrat de Mar (Catalan Meteorological Service, SMC). The average total irradiance of three days before each sampling date was used here.

2.2. Measured variables

For chlorophyll *a* determinations (Chl *a*), a sample volume of 150 mL was filtered through Whatman GF/F filters and subsequently extracted in acetone (90% v/v) in the dark at 4 °C for 24 h. The concentrations were determined fluorometrically with a Turner Designs fluorometer. For Chl *a* smaller than 3 μm we applied the same procedure to 250 mL water sample previously filtered through polycarbonate filters with a 3 μm pore size.

Samples for carbon content, absorption and fluorescence measurements of DOM were immediately processed after arriving into the laboratory. Samples were filtered through Whatman GF/F filters using an acid-cleaned glass filtration system. Approximately 10 mL of water was collected in pre-combusted (450 °C, 12 h) glass ampoules for dissolved organic carbon (DOC) determination. H_3PO_4 was added to acidify the sample to pH<2 and the ampoules were heat-sealed and stored in the dark at 4 °C until analysis. DOC was measured with a Shimadzu TOC-V CSH organic carbon analyser. The system was standardised daily with potassium hydrogen phthalate. Each ampoule was injected 3–5 times and the average area of the 3 replicates that yielded a standard deviation <1% was chosen to calculate the average DOC concentration of each sample after subtraction of the average area of the freshly-produced UV-irradiated milli-Q water used as a blank. Reference materials provided by Prof. D. Hansell (University of Miami) were analysed to test the performance of the analyser. A concentration of 45.2 ± 0.3 μmol C L^{-1} was obtained for the deep ocean reference (Sargasso Sea deep water, 2600 m) minus the blank reference materials. The nominal DOC value provided by the reference laboratory is 45 μmol C L^{-1}.

Samples for CDOM and FDOM determinations were measured by triplicate immediately after filtration, between 2 and 3 h after collection. CDOM absorption was measured in a Varian Cary spectrophotometer equipped with a 10 cm quartz cell. Spectral scans were collected between 250 and 750 nm at a constant room temperature of 20 °C. Milli-Q water was used as blank. The absorption coefficient at all wavelengths, $a_{CDOM}(\lambda)$ (in m^{-1}), was calculated as

$$a_{CDOM}(\lambda) = 23.03 \cdot [Abs(\lambda) - Abs(600-750)] \quad (1)$$

Where Abs(λ) is the absorbance at wavelength λ, and Abs(600–750) is the average absorbance between 600 and 750 nm, which corrects for the residual scattering by fine size particle fractions, micro-air bubbles or colloidal material present in the sample, or refractive index differences between the sample and the reference (in m^{-1}). The carbon specific absorption coefficient at 254 nm, $SUVA_{254}$ (Weishaar et al., 2003), was calculated dividing the decadic $a_{CDOM}(254)$ by the DOC concentration and expressed in m^2 mol C^{-1}. Following Helms et al. (2008), CDOM spectral slopes were calculated over two narrow wavelength ranges, $S(275–295)$ and $S(350–400)$, using linear regressions of the natural log-transformed $a_{CDOM}(\lambda)$ spectra. In addition, the dimensionless $S(275–295)/S(350–400)$ ratio, known as S_R, was also calculated.

CDOM induced fluorescence (FDOM) was determined with a LS 55 Perkin Elmer Luminescence spectrometer, equipped with a xenon discharge lamp, equivalent to 20 kW for 8 μs duration. The instrument has 2 monochromators that ranged between 200 and 800 nm for excitation wavelengths and between 200 and 900 nm for emission wavelengths. The detector was a red-sensitive R928 photomultiplier, and a photodiode worked as reference detector. Slit widths were fixed to 10 nm for the excitation and emission wavelengths and the scan speed was 250 nm min^{-1}. Measurements were performed at a constant room temperature of 20 °C in a 1 cm quartz fluorescence cell. Single measurements at specific excitation–emission wavelengths (Ex/Em) were performed. To compare with other studies, the wavelengths chosen for the Ex/Em pair measurements were those previously established by Coble (1996): 280 nm/350 nm (peak T) for protein-like substances; and 340 nm/440 nm (peak C) for humic-like substances absorbing in the UV-A. The fluorescence of UV-radiated Milli-Q at those Ex/Em pairs was subtracted from all samples. Factory-set excitation and emission corrections of the instruments were used. Since the absorption coefficients of all samples at any wavelength were <10 m^{-1}, it was not necessary to correct for inner filters effects (Stedmon and Bro, 2008). Following Coble (1996), the fluorescence intensities were expressed in quinine sulphate units (QSU) by calibrating the instrument at Ex/Em: 350 nm/450 nm against a quinine sulphate dihydrate (QS) standard made up in 0.05 mol L^{-1} sulphuric acid. Fluorescence intensities of peaks T and C in QSU have been named as $F(280/350)$ and $F(340/440)$, respectively.

Finally, the quantum yield of fluorescence at excitation 340 nm, $\Phi(340)$—i.e. the portion of the light absorbed by the DOM at 340 nm that is re-emitted as fluorescent light—was calculated by comparison to the fluorescence emission between 400 and 600 nm from the QS standard using the equation (Green and Blough, 1994):

$$\Phi(340) = \frac{F(400-600)}{a_{CDOM}(340)} \cdot \frac{a_{CDOM}(340)_{QS}}{F(400-600)_{QS}} \cdot \Phi(340)_{QS} \quad (2)$$

Where $a_{CDOM}(340)_{QS}$ is the absorption coefficient of the QS standard at 340 nm (in m^{-1}); $F(400–600)$ and $F(400–600)_{QS}$ are the average integrated fluorescence spectra between 400 and 600 nm at a fixed excitation wavelength of 340 nm (in QSU) of the sample and the QS standard, respectively; and $\Phi(340)_{QS}$ is the dimensionless fluorescence quantum yield of the QS standard, 0.54 according to Melhuish (1961).

Bacterial heterotrophic activity (BA) was estimated using the [^{3}H]-leucine (Leu) incorporation method (Kirchman et al., 1985) as in Alonso-Sáez et al. (2008). For each sample, triplicate or quadruplicate aliquots (1.2 m#) and one or two TCA killed controls were incubated with 40 nmol L^{-1} Leu for about 2 h at in situ temperature in the dark. The incorporation was stopped with the addition of 120 μL of cold TCA 50% and samples were kept frozen at 20 °C until processing, which was carried out by the centrifugation method. Finally, samples were counted on a Beckman scintillation counter 24 h after the addition of 1 mL of scintillation cocktail (Optiphase Hisafe2, Perkin-Elmer).

2.3. Harmonic analysis of the time series

To obtain the annual mean (b1), amplitude (b2) and diphase (b3) parameters defining the seasonal cycle of a variable (Y), a harmonic analysis of the annual component (period, 365 days) of each time series was performed using the Levenberg–Marquardt algorithms implemented in the STATISTICA software. We fitted the data of total irradiance, water temperature, salinity, DOC, Chl *a*, BA, $a_{CDOM}(254)$, $SUVA_{254}$, $S(275–295)$ and $S(350–400)$, S_R, $F(340/440)$, $F(280/350)$ and $\Phi(340)$ to the following trigonometric equation:

$$Y = b1 + b2 \cdot \cos\left(\frac{2\pi}{365} \cdot t + b3\right) \quad (3)$$

where t is the ordinal date (ranging from 1 to 365/366). The diphase parameter, b3, was expressed as the ordinal date at which each time series achieved the annual maximum value.

3. Results

3.1. Annual cycles of environmental variables

The harmonic Eq. (3) explained 86% of the variability (Table 1) of the time series of total irradiance in Blanes Bay (Fig. 1a). Maximum irradiances (295 ± 12 W m^{-2}) occurred by late June (day of the year 179 ± 4). Sea surface temperature followed also a well-defined annual cycle (Fig. 1b) that explains 90% of the variability of the time series with an average annual mean of 16.7 ± 0.2 °C (Table 1). The average annual minimum temperature, 11.4 ± 0.5 °C, occurred by mid February when maximum winter mixing happened, and the average annual maximum, 22.0 ± 0.5 °C, was recorded by mid August (day of the year, 231 ± 3), i.e. 52 ± 7 days later than the seasonal maximum of irradiance, when summer stratification was highest. Conversely, the annual cycle explained only 24% of the variability of the time series of salinity (Fig. 1c). Salinity was quite stable around the average annual mean of 37.97 ± 0.04, the amplitude being just 0.17 ± 0.05, except during a few particular dates associated with rainwater episodes. Maximum values were observed during autumn (mid November) and minimum during spring (mid May).

The seasonal cycle of total chlorophyll *a*, as modelled with Eq. (3), explained 41% of the variability of the time series (Fig. 1d; Table 1). The average annual mean was 0.63 ± 0.05 mg m^{-3} with average maximum values of 1.04 ± 0.13 mg m^{-3} by late February (day of the year, 54 ± 10) and minimum values of 0.22 ± 0.13 mg m^{-3} by late August. A similar seasonal cycle was observed for the fraction of Chl *a*<3 μm (Fig. 1e), but it explained 55% of the variability and reached the seasonal maximum significantly earlier, by late January (day of the year, 28 ± 8). The portion of the Chl *a* which was <3 μm was maximum (64 ± 5%) by late October (day of the year, 294 ± 20) and minimum (45 ± 5%) by late April (day of the year, 111 ± 20; Fig. 1e, solid line). The fitting of bacterial activity to Eq. (3) explained 36% of the variability, presenting an average maximum of 70 ± 9 pmol leu L^{-1} h^{-1} by mid July (day of the year, 198 ± 13) and a minimum of 8 ± 9 pmol leu L^{-1} h^{-1} by mid January (day of the year, 15 ± 13).

3.2. Annual cycles of the bulk and coloured fractions of DOM

DOC concentration and the optical properties of CDOM also followed statistically significant annual cycles that fit to Eq. (3). Seasonality explained 55% of the variability of DOC. The average annual mean concentration of DOC was 79 ± 2 μmol C L^{-1}; it accumulated in Blanes Bay from the average annual minimum of 63 ± 5 μmo C L^{-1} recorded by early March to the average annual maximum of 95 ± 5 μmol C L^{-1} by early September (day of the year, 247 ± 9; Fig. 2a, Table 1), about half a month later than the maximum of sea surface temperature. Note that these are the typical annual concentrations but higher values, reaching 140 μmol C L^{-1}, were sporadically recorded.

Fifty percent of the variability of the absorption coefficient at 254 nm, $a_{CDOM}(254)$, an indicator of the abundance of conjugated carbon double bounds (Lakowicz, 2006), was explained by Eq. (3). Although $a_{CDOM}(254)$ also accumulated through the spring and summer, the average annual maximum absorption of 1.77 ± 0.06 m^{-1}

Table 1
Fitting parameters (±standard error) of Eq. (3) for the time series of the studied variables: annual mean (b1), amplitude (b2) and diphase (b3). Coefficients b1 and b2 are expressed in the units of each variable and b3 is expressed in days of the year. R^2, determination coefficient; *n*, number of data of each time series; *p-level*, significance of the linear fitting for the measured versus the modelled data; SD res, standard error of the residuals of the measured minus the modelled data; Anal. err, analytical error of the experimental determination of each variable.

Variable	Annual mean (b1)	Amplitude (b2)	Seasonal max.(b3) (day of the year)	R^2	*n*	*p-level*	SD res	Anal. err
Irradiance (W m^{-2})	182 ± 5	113 ± 7	179 ± 4	0.86	43	<0.001	31	9
Temperature (°C)	16.7 ± 0.2	5.2 ± 0.3	231 ± 3	0.90	43	<0.001	1.2	0.01
Salinity	37.97 ± 0.04	0.17 ± 0.05	321 ± 19	0.24	43	<0.001	0.23	0.01
Total Chl*a* (mg m^{-3})	0.63 ± 0.05	0.41 ± 0.08	54 ± 10	0.41	42	<0.001	0.32	0.05
Chl*a*<3 μm (mg m^{-3})	0.33 ± 0.02	0.21 ± 0.03	28 ± 8	0.55	38	<0.001	0.12	0.05
BA (pmol leu L^{-1} h^{-1})	39 ± 5	31 ± 8	198 ± 13	0.36	31	<0.001	27	3.5
DOC (μmol L^{-1})	79 ± 2	16 ± 3	247 ± 9	0.55	38	<0.001	11	1
$a_{CDOM}(254)$ (m^{-1})	1.59 ± 0.02	0.18 ± 0.03	217 ± 10	0.50	31	<0.001	0.11	0.01
$SUVA_{254}$ (m^2 mol C^{-1})	8.9 ± 0.2	0.9 ± 0.3	96 ± 22	0.25	29	<0.024	2.5	0.2
$a_{CDOM}(254/365)$	14.8 ± 0.6	2.3 ± 0.9	249 ± 23	0.21	31	<0.005	2.8	2.7
$S(350–400)$ (nm^{-1})	0.0165 ± 0.0004	0.0019 ± 0.0006	210 ± 15	0.29	31	<0.001	0.0020	0.0004
$S(275–295)/S(350–400)$	2.02 ± 0.05	0.17 ± 0.07	21 ± 23	0.16	31	<0.015	0.26	0.07
$F(340/440)$ (QSU)	0.50 ± 0.02	0.12 ± 0.03	35 ± 10	0.38	41	<0.001	0.10	0.01
$F(280/350)$ (QSU)	1.09 ± 0.05	0.27 ± 0.07	255 ± 16	0.29	41	<0.001	0.28	0.03
$\Phi(340)$ (%)	0.63 ± 0.02	0.13 ± 0.03	23 ± 12	0.39	31	<0.001	0.11	0.08

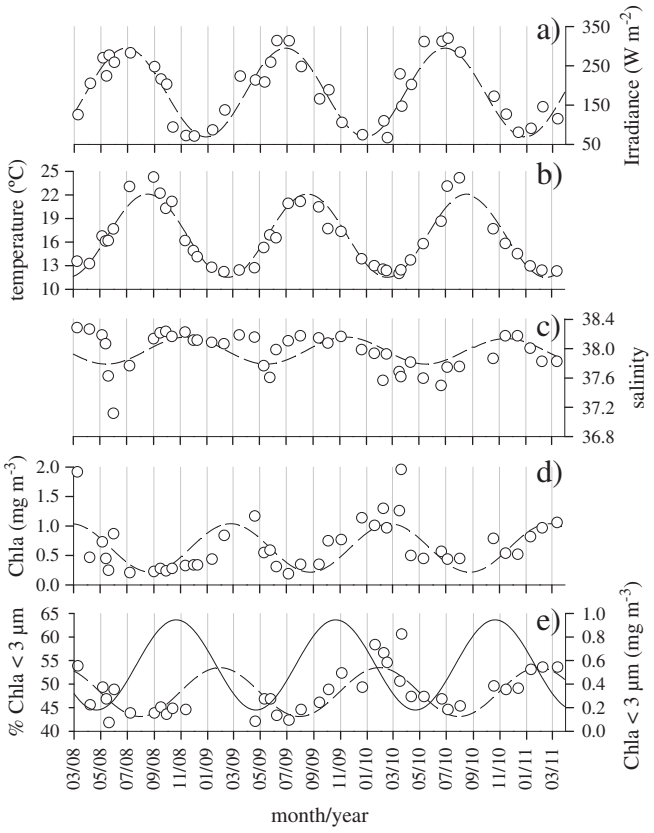

Fig. 1. Time series of a) total irradiance, b) temperature, c) salinity, d) chlorophyll *a* and e) chlorophyll *a*<3 µm. Modelled values (dotted line) and measured values (open dots). Solid line in plot e) corresponds to modelled values of % Chla<3.

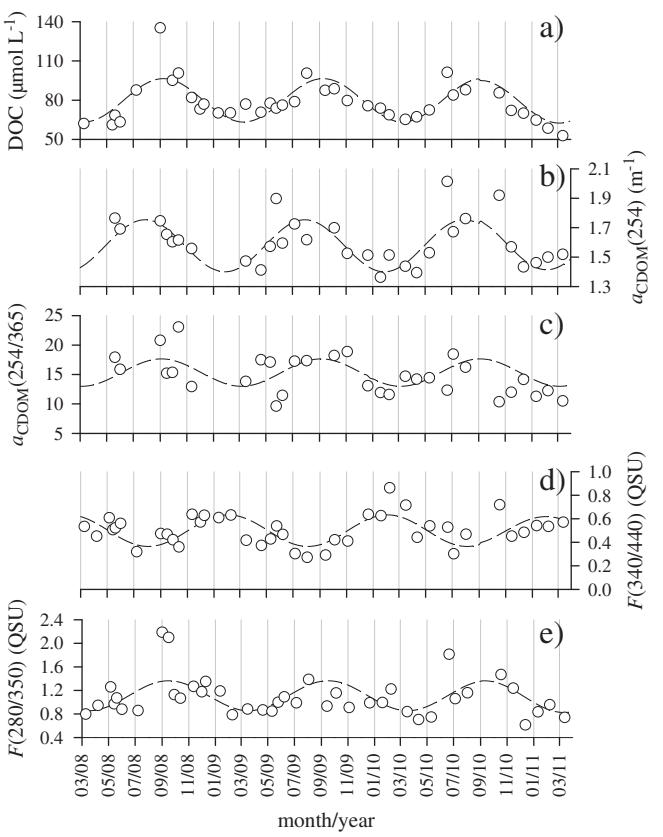

Fig. 2. Time series of a) DOC, b) $a_{CDOM}(254)$, c) $a_{CDOM}(254/365)$, d) peak C or $F(340/440)$ and e) peak T or $F(280/350)$. Modelled values (dotted line) and measured values (open dots).

(Fig. 2b) occurred by early August (day of the year, 217 ± 10), i.e. 30 ± 13 days before the annual maximum of DOC (Table 1). The diphase of DOC and $a_{CDOM}(254)$, led to an annual cycle of $SUVA_{254}$ that reaches the average annual maximum of 9.8 ± 0.3 m^2 mol C^{-1} by early April (day of the year, 96 ± 22). $SUVA_{254}$ is commonly used as an aromaticity index after Weishaar et al. (2003) found a good correlation between this variable and the percentage of aromaticity determined by ^{13}C NMR spectroscopy. Other useful indices are the absorption coefficient ratio at 254 nm to 365 nm, $a_{CDOM}(254/365)$ (Fig. 2c), which is inversely correlated with the DOM average molecular weight (Dahlén et al., 1996; Engelhaupt et al., 2003) or the spectral slope ratio, S_R, which is directly correlated to the molecular weight and the photochemically induced shifts in molecular weight (Helms et al., 2008). In our study, both variables described statistically significant annual cycles that explained 16–21% of the total variability of the time series and $a_{CDOM}(254/365)$ was in phase with the annual cycle of DOC and S_R with the annual cycles of $F(340/440)$ and $\Phi(340)$ (Table 1).

The fluorescence of humic-like substances absorbing in the UV-A region of the spectrum, $F(340/440)$, followed an annual cycle that explained 38% of the variability of the time series and was out of phase with $a_{CDOM}(254)$ and DOC. $F(340/440)$ evolved from an average annual maximum of 0.62 ± 0.04 QSU by early February (day of the year, 35 ± 10) to a minimum of 0.38 ± 0.04 QSU by early August (Fig. 2d). The time course of the fluorescence quantum yield at 340 nm, $\Phi(340)$, another aromaticity index (Birks, 1970; Turro, 1991), followed also a statistically significant seasonal cycle that explained 39% of the variability of the time series and was significantly in phase with $F(340/440)$ (Table 1). The average annual mean value of $\Phi(340)$ was 0.63 ± 0.02%, ranging from an average annual maximum of 0.76 ± 0.05% to an average annual minimum of 0.50 ± 0.05%. Conversely, the fluorescence of protein-like substances (Fig. 2e) followed an annual cycle that explained 29% of the variability of the time series and was in phase with DOC, reaching the annual maximum by early September (day of the year, 255 ± 16; Table 1).

3.3. Deseasonalised time series

The studied variables were deseasonalised by subtracting the annual cycles modelled with Eq. (3) (dotted lines in Figs. 1 and 2) from the original time series (open dots in Figs. 1 and 2). The deseasonalised time series of the fluorescence of the humic-like peak C, $\Delta F(340/440)$ (Fig. 3a), was generally opposite to the deseasonalised time series of salinity, ΔSal (Fig. 3b). In fact, a significant negative linear correlation ($R = -0.62$, $p < 0.001$, $n = 40$) existed between $\Delta F(340/440)$ and ΔSal (Fig. 4a). ΔSal was also negatively correlated with the aromaticity index $\Phi(340)$ ($R = -0.52$, $p < 0.05$, $n = 31$, Fig. 4b). On the other hand, the deseasonalised time series of the protein-like peak T, $\Delta F(280/350)$ (Fig. 3c), and that of the bulk DOC, ΔDOC (Fig. 3d), followed the same trend, presenting a significantly positive linear correlation ($R = 0.63$, $p < 0.001$, $n = 38$, Fig. 4c).

4. Discussion

The standard error of the values modelled with Eq. (3) (SD res in Table 1) was about one order of magnitude larger than the analytical error of the measurement (Anal. err in Table 1) for all study variables except $a_{CDOM}(254/365)$ and $\Phi(340)$, which were of the same magnitude. Therefore, the part of the variability not explained by the harmonic model ($1 - R^2$) was essentially due to environmental variability at time scales of frequency higher than the annual cycle modelled by Eq. (3). For the particular case of $a_{CDOM}(254/365)$ and $\Phi(340)$, the harmonic model was as good as the accuracy of the determination of these variables.

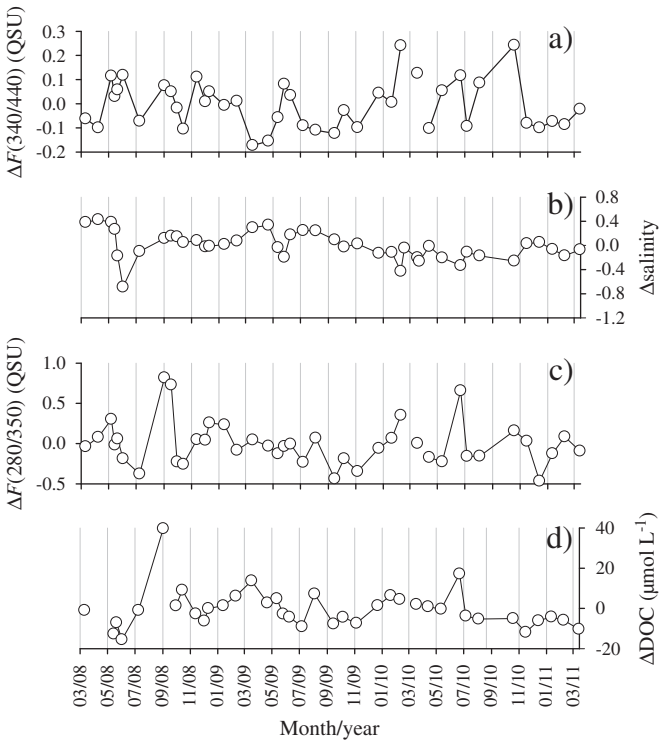

Fig. 3. Time series of the deseasonalized a) peak C or *F*(340/440), b) salinity, c) peak T or *F*(280/350) and d) DOC.

The Blanes Bay Microbial Observatory is representative of oligotrophic coastal ecosystems which sporadically receive nutrients and terrestrial carbon inputs during stormy periods (Guadayol et al., 2009). The annual cycle of sea surface temperature traces the seasonal evolution from winter mixing to summer stratification characteristic of temperate latitudes. The temperature range obtained in this work agrees with that reported elsewhere (Duarte et al., 1999). The average annual maximum concentration of Chl *a* was composed of 50% of chlorophyll in phytoplankton >3 μm and a 50% in phytoplankton<3 μm. This maximum occurred at the time of the average annual minimum of temperature as previously found by Guadayol et al. (2009). The development of this late winter phytoplankton bloom is one of the seasonal characteristics of Mediterranean phytoplankton communities (Duarte et al., 1999). Stratification of the water column throughout the spring and summer isolates the water of Blanes Bay from the subsurface offshore waters, preventing the flux of new inorganic nutrients into the bay, which leads to severe oligotrophic conditions (Alonso-Sáez et al., 2008). Nutrient concentrations during the summer season of the studied years were around 0.03 μmol L^{-1} for phosphate, 0.3 μmol L^{-1} for inorganic nitrogen, and 0.1 μmol L^{-1} for silicate (data not shown). The typical annual range of DOC concentrations recorded during the study period had previously been observed in Blanes Bay (Lucea et al., 2005; Alonso-Sáez et al., 2008; Vila-Reixach et al., 2012) as well as in other temperate marine ecosystems relatively unaffected by terrestrial inputs (Nelson et al., 1998; Álvarez-Salgado et al., 2001). The summer accumulation of DOC of 32 ± 9 μmol C L^{-1} observed in Blanes Bay is similar to that reported for the tropical station of the Hawaii Ocean Time Series (40 μmol C L^{-1}, http://hahana.soest.hawaii.edu/hot/) but doubles that of the Bermuda Atlantic Time Series Study site (15 μmol C L^{-1}, Nelson et al., 1998).

The dissolved organic materials traced by $a_{CDOM}(254)$ and peak T accumulated also in Blanes Bay during the summer but $a_{CDOM}(254)$ reached its annual maximum about one month before peak T that, in turn, was in phase with DOC. Therefore, the optical properties of CDOM allowed distinguishing the accumulation of two DOC pools which differ in their potential bioavailability. Among the by-products of microbial respiration there are compounds with conjugated carbon

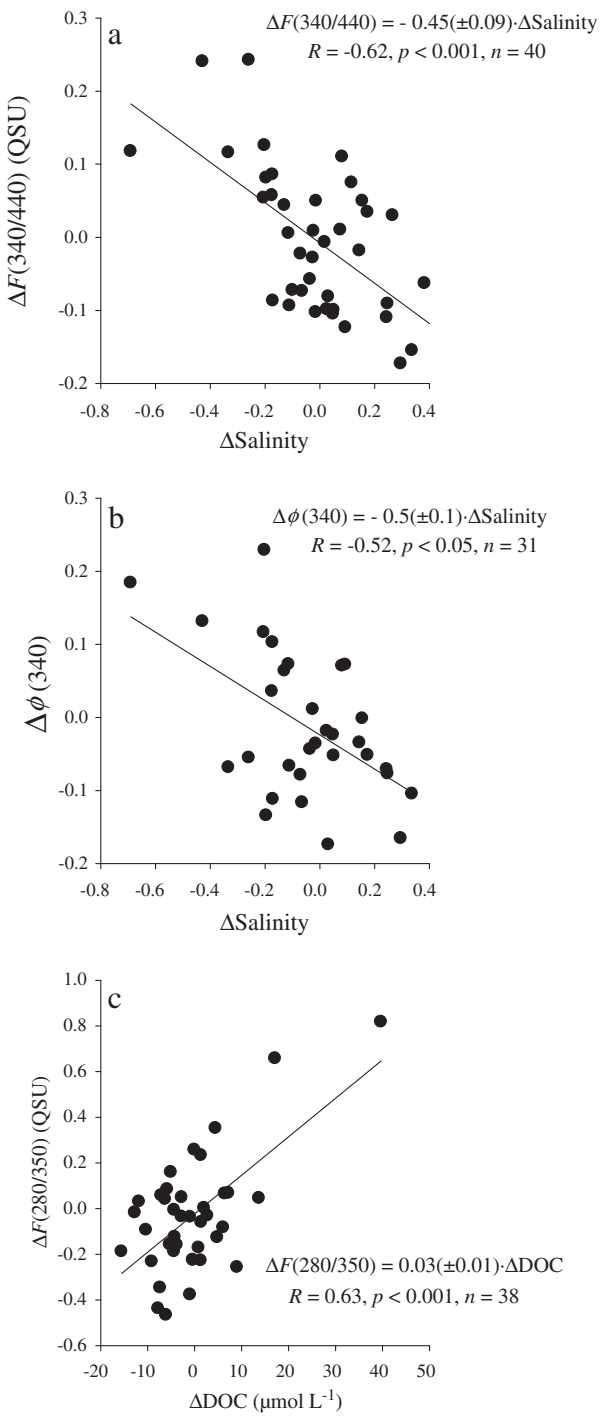

Fig. 4. Deseasonalized time series of a) peak C or *F*(340/440) versus salinity, b) *Φ*(340) versus salinity, and c) peak T or *F*(280/350) versus DOC.

double bonds that can be traced by $a_{CDOM}(254)$ since microorganisms produce fluorescent humic-like substances absorbing at around 260 nm and emitting at around 460 nm (Romera-Castillo et al., 2011a). This fluorescent maximum is within the range established by Coble (1996) for peak A (Ex/Em 260/400–460). The annual minimum of $a_{CDOM}(254)$ was recorded in winter likely because of mixing with the less coloured offshore waters. In this sense, Vila-Reixach et al. (2012) have recently shown that strong NW winds blowing from November to May, promote the offshore export of the DOC rich waters in the Bay. On the other hand, these authors found that DOC accumulated during spring and summer because of the increasing stratification and the prevalence of SE winds, which favours DOC accumulation into the

Bay. Moreover, there is a dominance of net production associated to microbial respiration over photochemical degradation in the stratified surface layer. In fact, the annual cycles of $a_{CDOM}(254)$ and bacterial activity were in phase, i.e. the annual maximum of both variables coincided in time. Our bacterial activity maximum also coincided with the bacterial respiration maximum previously reported in the same area (Duarte et al., 2004). Reduced photochemical degradation of substances absorbing at 254 nm also contributed to the summer accumulation of $a_{CDOM}(254)$ because the largest losses of fluorescence and absorbance occur at the same wavelengths at which the compounds are irradiated (Del Vecchio and Blough, 2002) and few photons of $\lambda<295$ nm reach the Earth's surface.

The fact that the annual cycle of peak T was in phase with DOC suggests that the DOC accumulated in Blanes Bay contained free and combined amino acids. In this sense, it is known that maintenance of the algal photosynthetic machinery after inorganic N and P exhaustion is accompanied by excretion of DOM and especially carbohydrates (Norman et al., 1995). P limitation in the Mediterranean could lead to the accumulation of protein materials of little use under P starvation, despite the fact that it would be labile in other (P replete) environments. Therefore, despite the potential lability of the exuded materials, P limitation would prevent their utilisation by heterotrophic bacteria leading to DOC accumulation in summer (Thingstad et al., 1997). DOM accumulation is a common process that has also been evidenced in other oligotrophic aquatic environments (e.g., Sargasso Sea, Thingstad et al., 1997; Siegel et al., 2002) as well as in experimental mesocosms (Norman et al., 1995). The accumulation of protein-like substances in summer was also observed in Florida Bay (Jaffé et al., 2008). Another plausible reason for the protein-like fluorescence maximum recorded in summer could be that photo-degradation of humic substances releases amino acid moieties or changes its position in the protein throughout conformational changes of the macromolecule, exhibiting higher fluorescence in that new form (Lakowic, 2006). This has been hypothesised in an experimental study where it was reported an increase of peak T after exposure of open ocean ultrafiltered DOM to sunlight (Romera-Castillo, et al., in prep.).

The annual cycle of the coloured and fluorescent humic-like substances that absorb natural light at wavelengths >300 nm, i.e. in the UV-B and UV-A range of the spectrum, is the result of the prevalence of consumption by photodegradation, over production by microbial respiration, of these materials (Coble, 2007). This pattern has been previously observed in other marine ecosystems relatively unaffected by continental runoff such as the oligotrophic BATS site (Nelson et al., 1998, 2004) or the eutrophic Iberian coastal upwelling system (Nieto-Cid et al., 2006; Romera-Castillo et al., 2011b) and it is the reason behind the relatively low values reported in the literature for the absorption coefficient (Nelson et al., 2010) and the induced fluorescence (Yamashita and Tanoue, 2008) of CDOM in surface ocean waters. Therefore, we hypothesise that the annual maximum accumulation of peak C, $F(340/440)$, was observed in winter as a result of three processes. First, the winter mixing of the waters into the bay with the more fluorescent waters offshore the bay. Given that peak C is degraded by sunlight, its fluorescence intensity increases significantly with depth. Therefore, the deeper the winter mixed layer the higher the fluorescence of peak C. The winter mixed layer in the offshore waters deepens to around 100 m (D'Ortenzio et al., 2005) whereas maximum depth at the Blanes Bay Microbial Observatory is 22 m. Second, the production of peak C by the community associated to the Chl $a<3$ μm, which peaked in late January, in phase with $F(340/440)$. Note that cyanobacteria and micromonas produce fluorescent DOM that peaks at $F(340/440)$ (Romera-Castillo et al., 2011a) and the smaller size fraction of phytoplankton in Blanes Bay is mainly composed on cyanobacteria, during summer, and micromonas, during winter (unpub. data). And third, photobleaching during spring and summer in the stratified waters of the bay. In fact, the seasonal minimum of $F(340/440)$ (day 218 ± 10) occurred in between the seasonal maxima of total irradiance (39 ± 11 days before) and temperature (14 ± 10 days after), i.e. in between the seasonal maxima of UV radiation and water column stratification.

The 39% reduction of $F(340/440)$ in Blanes Bay from the annual maximum in early February to the annual minimum in early August was close to those reported in the Middle Atlantic Bight (~30%, Vodacek and Blough, 1997) and in the eutrophic coastal system of the Ría de Vigo (40–50%, Nieto-Cid et al., 2006). Photobleaching of humic-like materials produces a dramatic loss of aromaticity and a decrease of the molecular weight of the irradiated materials (Moran and Zepp, 1997; Osburn et al., 2001). Coherently, our annual cycles of the aromaticity indices $SUVA_{254}$ and $\Phi(340)$ and the average molecular weight indices $a_{CDOM}(254/365)$ and S_R agree with the photodegradation of aromatic and high molecular weight compounds during summer to generate colourless, more aliphatic and lower molecular weight organic products, as well as CO and CO_2 (Moran and Zepp, 1997). Therefore, the fraction of CDOM that reaches maximum concentrations by mid-September seems to be of relatively lower average molecular weight and aromaticity than the CDOM accumulated during the winter. Although labile compounds are formed during photodegradation processes (Moran and Zepp, 1997; Obernosterer et al., 1999), the previously referred inability of the microbial loop led to the accumulation of these materials in the stratified surface layer.

Although direct comparison of spectral slopes is not an easy task because different wavelength ranges were used by different authors, it can be reported that the absorption spectral slopes obtained in Blanes Bay are relatively high when compared with the values reported for surface waters of the Gulf of Lions (Ferrari, 2000) and for the Bay of Marseille (Para et al., 2010), both in the NW Mediterranean Sea, or for an eutrophic coastal embayment as the Ría de Vigo (Romera-Castillo et al., 2011b). In Blanes, as in Marseille, absorption spectral slopes are relatively lower during winter than in summer (Para et al., 2010) as a consequence of a photo-degradation increase during summer, characteristic of temperate latitudes. Continental CDOM inputs tend to decrease spectral slopes, while photodegradation processes tend to rise them (Del Vecchio and Blough, 2004; Nelson et al., 2010). Since natural irradiation is not much different between both Mediterranean and Atlantic studied sites, with average values of around 160–180 W m^{-2} (Ruiz et al., 2008; www.meteogalicia.es), the reason behind the relatively higher values of S in Blanes Bay is likely because it has less terrestrial influence than the Bay of Marseille or the Ría de Vigo. The former is close to the major source of freshwater and terrigenous particles of the NW Mediterranean Sea (Rhône River; Sempéré et al., 2000) and the Ría de Vigo directly receives Oitaben-Verdugo river waters with an average annual flow of 15 m^3 s^{-1} (Nogueira et al., 1997).

The annual mean ± amplitude of the fluorescence quantum yield at 340 nm found in Blanes Bay, 0.63 ± 0.12%, is within the range of values reported for the Gulf of Lions but lower than the average recorded in the more eutrophic Rhône river plume (0.96%; Ferrari, 2000) and Ría de Vigo (0.91 ± 0.30%; Romera-Castillo et al., 2011b). Laboratory experiments have shown that photobleaching produces a decrease of the fluorescence quantum yield, while microbial degradation produces an increase (De Haan, 1993; Lønborg et al., 2010). Therefore, the differences in $\Phi(340)$ values found in oligotrophic and eutrophic sites can be explained as a consequence of higher microbial degradation activities in the latter sites. Moreover, the terrestrial materials associated to the Rhône River plume could also contribute to increase $\Phi(340)$, since terrestrial organic matter presents a higher degree of aromaticity than marine organic matter does (Repeta et al., 2002; Benner, 2003).

The seasonal cycle of the fluorescent humic-like substances is disrupted by the episodic arrival of continental waters to the sampling site, which can be traced by a salinity decrease (Fig. 1c). Lower salinities are usually accompanied by higher values of $F(340/$

440) (Fig. 2d); in fact, a significant negative correlation was observed between the deseasonalised time series of salinity and those of $F(340/440)$ (Fig. 4a) and $\Phi(340)$ (Fig. 4b). This is, again, because continental waters are richer in humic-like fluorescent compounds with respect to marine waters (Coble, 1996; Repeta et al., 2002; Benner, 2003). The $F(340/440)$ measured at the mouth of River Tordera, placed south of the sampling site, on 15/05/2008 was as high as 53 QSU while DOC and total inorganic N values were of 263 μmol L^{-1} C and 90.3 μmol L^{-1}, respectively (unpub. data). Furthermore, continental runoff also transports new inorganic nutrients to the sampling site that can contribute to enhance microbial activity, which is known to also produce humic-like substances (Nieto-Cid et al., 2006; Lønborg et al., 2010; Romera-Castillo et al., 2010, 2011a). Coherently, the major determining factors for the interannual differences in microplankton metabolism are the variability in rainfall and continental runoff (Satta et al., 1996; Guadayol et al., 2009). The fact that the marked salinity decrease observed in June 2008 was not accompanied by a large increase of $F(340/440)$ could be due to photodegradation of continental humic substances during water advection to the sampling site and/or a delay in the stimulation of microbes by nutrients transported by continental waters.

Absorption and fluorescence spectroscopy measurements of CDOM at the Blanes Bay Microbial Observatory have allowed distinguishing between three DOM pools of different origin and photo- and biolability. We show that the optical properties of DOM, which are simple, fast and relatively inexpensive to measure, can be incorporated in monitoring sampling programs as a complement to DOC measurements as they provide useful information about the physical and biogeochemical processes controlling the stocks and the reactivity of the DOM pool.

Acknowledgements

We thank Vanessa Balagué, Clara Cardelús and Irene Forn for organizing sampling at Blanes Bay and for the basic oceanographic data, Encarna Borrull for technical assistance, Clara Ruiz and Ana Gomes for their help with bacterial activity measurements, and the Nutrient Analysis Service of the Institut de Ciències del Mar-CSIC. This study was funded by an I3P-predoctoral fellowship to C.R.-C. from the Consejo Superior de Investigaciones Científicas (CSIC) within the projects: MODIVUS (CTM2005-04795/MAR), SUMMER (CTM2008-03309/MAR) and STORM (CTM2009-09352). Finally, we owe thanks to Colin Stedmon and one anonymous reviewer for their comments, which have improved this work.

References

Alonso-Sáez, L., Vázquez-Domínguez, E., Cardelús, C., Pinhassi, J., Sala, M.M., Lekunberri, I., Balagué, V., Vila-Costa, M., Unrein, F., Massana, R., Simó, R., Gasol, J.M., 2008. Factors controlling the year-round variability in carbon flux through bacteria in a coastal marine system. Ecosystems 11, 397–409.

Álvarez-Salgado, X.A., Gago, J., Miguez, B.M., Perez, F.F., 2001. Net Ecosystem Production of Dissolved Organic Carbon in a Coastal Upwelling System: The Ria de Vigo, Iberian Margin of the North Atlantic. Limnol. Oceanogr. 46, 135–147.

Benner, R., 2003. Molecular indicators of the Bioavailability of Dissolved Organic Matter. In: Findlay, S., Sinsabaugh, R. (Eds.), Aquatic Ecosystems: Interactivity of Dissolved Organic Matter. Academic Press, pp. 121–137.

Birks, J.B., 1970. Photophysics of aromatic molecules. Willey-Interscience, London.

Coble, P.G., 1996. Characterization of marine and terrestrial DOM in seawater using excitation–emission matrix spectroscopy. Mar. Chem. 51, 325–346.

Coble, P.G., 2007. Marine optical biogeochemistry: the chemistry of ocean color. Chem. Rev. 107, 402–418.

D'Ortenzio, F., Iudicone, D., De Boyer Montegut, C., Testor, P., Antoine, D., Marullo, S., Santoleri, R., Madec, G., 2005. Seasonal variability of the mixed layer depth in the Mediterranean Sea as derived from in situ profiles. Geophys. Res. Lett. 32, L12605.

Dahlén, J., Bertilsson, S., Pettersson, C., 1996. Effects of UV-A irradiation on dissolved organic matter in humic surface waters. Environ. Int. 22, 501–506.

De Haan, H., 1993. Solar UV-light penetration and photodegradation of humic substances in peaty lake water. Limnol. Oceanogr. 38, 1072–1076.

Del Castillo, C.E., Coble, P.G., Morell, J.M., López, M.J., Corredor, J.E., 1999. Analysis of the optical properties of the Orinoco River plume by absorption and fluorescence spectroscopy. Mar. Chem. 66, 35–51.

Del Vecchio, R., Blough, N.V., 2002. Photobleaching of chromophoric dissolved organic matter in natural waters: kinetics and modeling. Mar. Chem. 78, 231–253.

Del Vecchio, R., Blough, N.V., 2004. Spatial and seasonal distribution of chromophoric dissolved organic matter and dissolved organic carbon in the Middle Atlantic Bight. Mar. Chem. 89, 169–187.

Duarte, C.M., Agustí, S., Kennedy, H., Vaqué, D., 1999. The Mediterranean climate as a template for Mediterranean marine ecosystems: the example of the northeast Spanish littoral. Prog. Oceanogr. 44, 245–270.

Duarte, C.M., Agustí, S., Vaqué, D., 2004. Controls on planktonic metabolism in the Bay of Blanes, Northwestern Mediterranean Littoral. Limnol. Oceanogr. 49, 2162–2170.

Engelhaupt, E., Bianchi, T.S., Wetzel, R.G., Tarr, M.A., 2003. Photochemical transformations and bacterial utilization of high-molecular-weight dissolved organic carbon in a southern Louisiana tidal stream (Bayou Trepagnier). Biogeochemistry 62, 39–58.

Ferrari, G.M., 2000. The relationship between chromophoric dissolved organic matter and dissolved organic carbon in the European Atlantic coastal area and in the West Mediterranean Sea (Gulf of Lions). Mar. Chem. 70, 339–357.

Galand, P., Gutiérrez-Provecho, C., Massana, R., Gasol, J.M., Casamayor, E.O., 2010. Interannual recurrence of archaeal assemblages in the coastal NW Mediterranean Sea (Blanes Bay Microbial Observatory). Limnol. Oceanogr. 55, 2117–2125.

Gasol, J.M., del Giorgio, P.A., Massana, R., Duarte, C.M., 1995. Active versus inactive bacteria: size-dependence in a coastal marine plankton community. Mar. Ecol. Prog. Ser. 128, 91–97.

Green, S.A., Blough, N.V., 1994. Optical absorption and fluorescence properties of chromophoric dissolved organic matter in natural waters. Limnol. Oceanogr. 39, 1903–1916.

Guadayol, Ò., Peters, F., Marrasé, C., Gasol, J.M., Roldán, C., Berdalet, E., Massana, R., Sabata, A., 2009. Episodic meteorological and nutrient-load events as drivers of coastal planktonic ecosystem dynamics: a time-series analysis. Mar. Ecol. Prog. Ser. 381, 139–155.

Helms, J.R., Stubbins, A., Ritchie, J.D., Minor, E.C., Kieber, D.J., Mopper, K., 2008. Absorption spectral slopes and slope ratios as indicators of molecular weight, source, and photobleaching of chromophoric dissolved organic matter. Limnol. Oceanogr. 53, 955–969.

Herndl, G.J., Muller-Niklas, G., Frick, J., 1993. Major role of ultraviolet-B in controlling bacterioplankton growth in the surface layer of the ocean. Nature 361, 717–719.

Jaffé, R., McKnight, D., Maie, N., Cory, R., McDowell, W.H., Campbell, J.L., 2008. Spatial and temporal variations in DOM composition in ecosystems: the importance of long-term monitoring of optical properties. J. Geophys. Res. 113, G04032.

Kieber, R.J., Hydro, L.H., Seaton, P.J., 1997. Photooxidation of triglycerides and fatty acids in seawater: implication toward the formation of marine humic substances. Limnol. Oceanogr. 42, 1454–1462.

Kirchman, D.L., K'nees, E., Hodson, R., 1985. Leucine incorporation and its potential as a measure of protein synthesis by bacteria in natural aquatic ecosystems. Appl. Environ. Microbiol. 49, 599–607.

Kirk, J.T.O., 1994. Light and Photosynthesis in Aquatic Ecosystems, 2nd edn. Cambridge University Press, Cambridge.

Kramer, G.D., Herndl, G.J., 2004. Photo- and bioreactivity of chromophoric dissolved organic matter produced by marine bacterioplankton. Aquat. Microb. Ecol. 36, 239–246.

Lakowic, J.R., 2006. Principles of Fluorescence Spectroscopy. Springer, Baltimore.

Lønborg, C., Álvarez-Salgado, X.A., Davidson, K., Martínez-García, S., Teira, E., 2010. Assessing the microbial bioavailability and degradation rate constants of dissolved organic matter by fluorescence spectroscopy in the coastal upwelling system of the Ría de Vigo. Mar. Chem. 119, 121–129.

Lucea, A., Duarte, C.M., Agustí, S., Kennedy, H., 2005. Nutrient dynamics and ecosystem metabolism in the Bay of Blanes (NW Mediterranean). Biogeochemistry 73, 303–323.

Margalef, R., 1945. Fitoplancton nerítico de la Costa Brava catalana (Sector de Blanes). Publ. Biol. Mediterr. 1, 1–48.

Melhuish, W.H., 1961. Quantum efficiencies of fluorescence of organic substances: effect of solvent and concentration of the fluorescent solute. J. Phys. Chem. 65, 229–235.

Moran, M.A., Zepp, R.G., 1997. Role of photoreactions in the formation of biologically labile compounds from dissolved organic matter. Limnol. Oceanogr. 42, 1307–1316.

Moran, M.A., Sheldon, W.M., Zepp, R.G., 2000. Carbon loss and optical property changes during long-term photochemical and biological degradation of estuarine dissolved organic matter. Limnol. Oceanogr. 45, 1254–1264.

Nelson, N.B., Siegel, D.A., Michaels, A.F., 1998. Seasonal dynamics of colored dissolved material in the Sargasso Sea. Deep Sea Res. I 45, 931–957.

Nelson, N.B., Carlson, C.A., Steinberg, D.K., 2004. Production of chromophoric dissolved organic matter by Sargasso Sea microbes. Mar. Chem. 89, 273–287.

Nelson, N.B., Siegel, D.A., Carlson, C.A., Swan, C.M., 2010. Tracing global biogeochemical cycles and meridional overturning circulation using chromophoric dissolved organic matter. Geophys. Res. Lett. 37, L03610.

Nieto-Cid, M., Álvarez-Salgado, X.A., Pérez, F.F., 2006. Microbial and photochemical reactivity of fluorescent dissolved organic matter in a coastal upwelling system. Limnol. Oceanogr. 51, 1391–1400.

Nogueira, E., Pérez, F.F., Ríos, A.F., 1997. Seasonal and long-term trends in an estuarine upwelling ecosystem (Ría de Vigo, NW Spain). Estuar. Coast. Shelf Sci. 44, 285–300.

Norman, B., Zweifel, U.L., Hopkinson, C.S., Fry, B., 1995. Production and utilization of dissolved organic carbon during an experimental diatom bloom. Limnol. Oceanogr. 40, 898–907.

Obernosterer, I., Reitner, B., Herndl, G.J., 1999. Contrasting effects of solar radiation on dissolved organic matter and its bioavailability to marine bacterioplankton. Limnol. Oceanogr. 44, 1645–1654.

Osburn, C.L., Morris, D.P., Thorn, K.A., Moeller, R.E., 2001. Chemical and optical changes in freshwater dissolved organic matter exposed to solar radiation. Biogeochemistry 54, 251–278.

Para, J., Coble, P.G., Charrière, B., Tedetti, M., Fontana, C., Sempéré, R., 2010. Fluorescence and absorption properties of chromophoric dissolved organic matter (CDOM) in coastal surface waters of the Northwestern Mediterranean Sea (Bay of Marseilles, France). Biogeosciences 7, 4083–4103.

Repeta, D.J., Quan, T.M., Aluwihare, L.I., Accardi, A., 2002. Chemical characterization of high molecular weight dissolved organic matter in fresh and marine waters. Geochim. Cosmochim. Acta 66, 955–962.

Romera-Castillo, C., Sarmento, H., Álvarez-Salgado, X.A., Gasol, J.M., Marrasé, C., 2010. Production of chromophoric dissolved organic matter by marine phytoplankton. Limnol. Oceanogr. 55, 446–454.

Romera-Castillo, C., Sarmento, H., Álvarez-Salgado, X.A., Gasol, J.M., Marrasé, C., 2011a. Net production/consumption of fluorescent coloured dissolved organic matter by natural bacterial assemblages growing on marine phytoplankton exudates. Appl. Environ. Microbiol. 77, 7490–7498.

Romera-Castillo, C., Nieto-Cid, M., Castro, C.G., Marrasé, C., Largier, J., Barton, E.D., Álvarez-Salgado, X.A., 2011b. Fluorescence: absorption coefficient ratio — tracing photochemical and microbial degradation processes affecting coloured dissolved organic matter in a coastal system. Mar. Chem. 125, 26–38.

Ruiz, S., Gomis, D., Sotillo, M.G., Josey, S.A., 2008. Characterization of surface heat fluxes in the Mediterranean Sea from a 44-year high-resolution atmospheric data set. Global Planet. Change 63, 258–274.

Satta, M.P., Agustí, S., Mura, M.P., Vaqué, D., Duarte, C.M., 1996. Microplankton respiration and net community metabolism in a bay on the NW Mediterranean coast. Aquat. Microb. Ecol. 10, 165–172.

Sempéré, R., Charrière, B., Van Wambeke, F., Cauwet, G., 2000. Carbon inputs of the Rhône River to the Mediterranean Sea: Biogeochemical implications. Global Biogeochem. Cycles 14, 669–681.

Siegel, D.A., Maritorena, S., Nelson, N.B., 2002. Global distribution and dynamics of colored dissolved and detrital organic materials. J. Geophys. Res. 107, C12. http://dx.doi.org/10.1029/2001JC000965.

Smith, R.C., Cullen, J.J., 1995. Effect of UV radiation on phytoplankton. Rev. Geophys. 33, 1211–1223.

Stedmon, C.A., Álvarez-Salgado, X.A., 2011. Shedding light on a black box: UV–visible spectroscopic characterization of marine dissolved organic matter. In: Jiao, N., Azam, F., Sanders, S. (Eds.), Microbial Carbon Pump in the Ocean. Science AAA/S, pp. 62–63.

Stedmon, C.A., Bro, R., 2008. Characterizing dissolved organic matter fluorescence with parallel factor analysis: a tutorial. Limnol. Oceanogr. Methods 6, 572–579.

Thingstad, T.F., Hagström, A., Rassoulzadegan, F., 1997. Accumulation of degradable DOC in surface waters: is it caused by a malfunctioning microbial loop? Limnol. Oceanogr. 42, 398–404.

Turro, N.J., 1991. Modern Molecular Photochemistry. University Science Books, Sausalito, CA.

Vila-Reixach, G., Gasol, J.M., Cardelús, C., Vidal, M., 2012. Seasonal dynamics and net production of dissolved organic carbon in an oligotrophic coastal environment. Mar. Ecol. Prog. Ser. 456, 7–19.

Vodacek, A., Blough, N.V., 1997. Seasonal variation of CDOM in the Middle Atlantic Bight: terrestrial inputs and photooxidation. Proceedings of SPIE-The International Society for Optical Engineering, 2963, pp. 132–137.

Weishaar, J.L., Aiken, G.R., Bergamaschi, B.A., Fram, M.S., Fujii, R., Mopper, K., 2003. Evaluation of specific ultraviolet absorbance as an indicator of the chemical composition and reactivity of dissolved organic carbon. Environ. Sci. Technol. 37, 4702–4708.

Yamashita, Y., Tanoue, E., 2008. Production of bio-refractory fluorescent dissolved organic matter in the ocean interior. Nat. Geosci. 1, 579–582.